Neuron, Vol. 20, 221–233, February, 1998, Copyright ©1998 by Cell Press

Neurotactin Functions in Concert with Other Identified CAMs in Growth Cone Guidance in *Drosophila*

Stephan Speicher,* Luis García-Alonso,*
Ana Carmena, María D. Martín-Bermudo,†
Santiago de la Escalera, Fernando Jiménez‡
Centro de Biología Molecular
"Severo Ochoa" (C.S.I.C.-U.A.M.)
Universidad Autónoma
28049 Madrid
Spain

Summary

We have isolated and characterized mutations in *Drosophila neurotactin*, a gene that encodes a cell adhesion protein widely expressed during neural development. Analysis of both loss and gain of gene function conditions during embryonic and postembryonic development revealed specific requirements for *neurotactin* during axon outgrowth, fasciculation, and guidance. Furthermore, embryos of some double mutant combinations of *neurotactin* and other genes encoding adhesion/signaling molecules, including *neuroglian*, *derailed*, and *kekkon1*, displayed phenotypic synergy. This result provides evidence for functional cooperativity in vivo between the adhesion and signaling pathways controlled by *neurotactin* and the other three genes.

Introduction

Cell adhesion proteins constitute a major functional class of molecules that are instrumental to the mechanisms controlling neurite outgrowth, growth cone guidance, and axon fasciculation (Goodman and Shatz, 1993; Keines and Cook, 1995; reviewed by Goodman, 1996). The functions of neural cell adhesion molecules (CAMs) in vertebrates have been inferred mainly from their patterns of expression and from in vitro assays (reviewed by Hynes and Lander, 1992; Rutishauser, 1993). These studies have revealed that neural CAMs frequently act as contact-mediated attractive, as well as repulsive, signals that operate by interaction with the cytoskeleton of the growth cone and via signal transduction mechanisms (e.g., see reviews by Doherty and Walsh, 1994; Tanaka and Sabry, 1995). Despite this, genetic analysis to evaluate the in vivo role of CAMs in neural development has led to unexpected results. Knockouts of different mouse genes encoding CAMs result in much milder phenotypes in guidance and connectivity than those expected from in vivo localization or in vitro analysis (Müller and Kypta, 1995; reviewed by Goodman, 1996; Hynes, 1996). Similarly, in *Drosophila*, loss-of-function mutations of different genes encoding CAMs (formally defined as membrane proteins capable of mediating aggregation of transfected S2 cells) cause little or no overt phenotypes, particularly in the CNS. Some CAM-encoding genes for which a mutational analysis has been reported in *Drosophila* are *neuroglian* (*nrg*; Bieber et al., 1989; Grenningloh et al., 1990; Hall and Bieber, 1997), *Fasciclin II* (*FasII*; Grenningloh et al., 1991; Lin and Goodman, 1994), *Fasciclin III* (*FasIII*; Chiba et al., 1995), *neuromusculin* (*nrm*; Kania and Bellen, 1995), *klingon* (Butler et al., 1997), and *irreC-rst* (Ramos et al., 1993), all of which encode CAMs of the immunoglobulin superfamily, and others like *Fasciclin I* (*FasI*; Elkins et al., 1990), *connectin* (Nose et al., 1994), and *pollux* (*plx*, Zhang et al., 1996). The lack of severe phenotypes in the absence of any single CAM has led to the proposal that during growth cone steering, either multiple recognition and signaling pathways have partially overlapping functions, or compensatory mechanisms result in the up-regulation of related genes, or both. As a consequence, inactivation of a single pathway does not lead to pronounced morphological abnormalities. In accordance with this proposal, the synergistic phenotype in the CNS of embryos lacking both Fas I and the *Drosophila* homolog of the cytoplasmic tyrosine kinase Abelson (Abl) suggested that the two proteins are part of different but functionally related pathways, either of which may suffice for axon guidance (Elkins et al., 1990). Likewise, the analysis of double mutants lacking two *Drosophila* receptor tyrosine phosphatases (RPTPs), DPTP69D and DPTP99A, indicated that these proteins have partially overlapping functions in motor neuron axon guidance (Desai et al., 1996). The molecular structures of these two RPTPs resemble that of some CAMs, suggesting that they, like some vertebrate CAMs, may also have adhesive properties (reviewed by Brady-Kalnay and Tonks, 1995; Fashena and Zinn, 1995). However, direct genetic evidence of functional overlap between neural CAMs, particularly in the CNS, is lacking.

Another important question is raised by the disparity in the patterns of expression of different CAMs. Some are expressed in highly restricted patterns, whereas the domain of expression of other CAMs is very broad. It might seem that the latter kind of pattern is not compatible with an instructive role in growth cone guidance.

Neurotactin (Nrt), a member of the serine esterase superfamily, is a type 2 cell surface glycoprotein with a single transmembrane domain (de la Escalera et al., 1990; Hortsch et al., 1990b). Like some other members of this group, e.g., *Drosophila* Gliotactin and Glutactin and rat Neuroligins (Olson et al., 1990; Auld et al., 1995; Ichtchenko et al., 1995, 1996), the extracellular esterase-homologous domain of Nrt lacks the serine residue required for enzymatic activity. The accumulation of Nrt at sites of contact between cells in vivo and in vitro, and its capacity to promote cell adhesion in tissue culture, strongly suggest that Nrt functions as a CAM (Barthalay et al., 1990; de la Escalera et al., 1990; Hortsch et al., 1990b; Darboux et al., 1996). Nrt is widely expressed in the CNS during stages of cell proliferation and differentiation and in the PNS in a more restricted fashion, suggesting a role during neural development. To test this presumptive function, we isolated *nrt* mutations and

*These authors contributed equally to this work.
†Present address: Wellcome/CRC Institute, Cambridge CB2 1QR, UK.
‡To whom correspondence should be addressed.

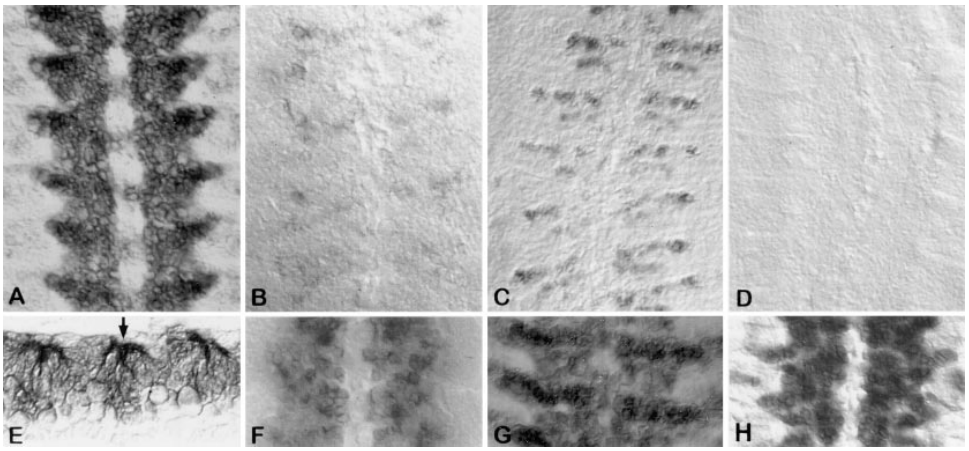

Figure 1. Expression of Nrt in the CNS of Wild-Type and Mutant Alleles

Different levels of Nrt accumulation are observed in wild-type (A), *nrt*^{1} (B), and *nrt*^{rP668} (C) stage 14 embryos stained with mAb 43B5 under the same conditions. Extended periods of staining reveal in *nrt*^{1} (F) and *nrt*^{rP668} (G) similar wide patterns of expression as in the wild type. No protein is detected in *nrt*^{5} null embryos (D). (E) is a saggital view of three consecutive segments from a stage 12 wild-type embryo embedded in wax and stained with mAb 43B5 after sectioning; Nrt accumulation in commissural axons (arrow) is evident. (H) shows Nrt expression in the CNS of a stage 14 embryo of the genotype *UAS–nrt*/+; *GAL4*^{Mz1277} *nrt*^{5}/*nrt*^{5}.

studied their effect upon axogenesis, both alone and in combination with mutations in other CAM and related genes. Lack of *nrt* produces mild but consistent defects in axogenesis in embryonic and postembryonic development. Ectopic expression of *nrt* causes axon misguidance phenotypes in the adult PNS. Furthermore, double mutant embryos for *nrt* and some CAM or CAM-like genes, mutations that lack obvious defects in axon pathfinding, display severe disruptions of the CNS axonal pattern.

Results

Wild-Type Expression of Neurotactin

A description of Nrt expression has been reported previously (de la Escalera et al., 1990; Hortsch et al., 1990b). We now extend the analysis to aspects of the expression pattern relevant to the present study. Nrt accumulates in the membranes of neuroblasts and their progeny (data not shown). Between stages 12 and 16 of axogenesis, extensive protein accumulation is observed in the CNS (Figure 1A). Analysis of serial sections revealed strong accumulation of Nrt in growing axon tracts and some heterogeneity in its distribution throughout the cell cortex (Figure 1E) but not in the motor axons exiting the CNS (data not shown). It was not possible to resolve Nrt in growth cones because of its widespread accumulation in cell bodies. After completion of neurogenesis, Nrt is down-regulated during the first larval instar (data not shown).

In the PNS of the embryo, Nrt was detected only in polyinnervated sensory organs (Barthalay et al., 1990; de la Escalera et al., 1990). In the developing PNS of the pupae, Nrt is expressed by ocellar pioneer neurons (Figure 3B) but not by neurons of neighbor bristles, which are monoinnervated sensory organs. Nrt is also expressed by differentiating eye photoreceptors (Barthalay et al., 1990; de la Escalera et al., 1990) and some sensory neurons in the wing (data not shown).

Isolation and Characterization of *neurotactin* Mutant Alleles

A mutant allele, *nrt*^{1}, was isolated after immunoscreening the embryonic F2 generation of a diepoxibutane (DEB) mutagenesis with anti-Nrt monoclonal antibody (mAb) 43B5 (see Experimental Procedures). Using Southern blot analysis and PCR, *nrt*^{1} DNA was found to lack a fragment of 103 bp within the region encoding the extracellular, C-terminal domain of the protein (Figure 2A). Due to the frameshift introduced by the deletion, the 234 C-terminal amino acids are substituted by an unrelated amino acid sequence in the Nrt^{1} protein (Figure 2B). mAb 43B5, which recognizes a cytoplasmic N-terminal epitope (de la Escalera et al., 1990), stains *nrt*^{1} embryos only very faintly (Figures 1B and 1F), although the level of transcription of the gene is normal (data not shown). Also, mAb 43B5 does not detect the mutant protein in Western blots (data not shown) as it does with the normal protein (de la Escalera et al., 1990), suggesting that Nrt^{1} is very unstable or its antigenicity is strongly reduced. Homozygous *nrt*^{1} flies are viable and fertile.

A homozygous viable enhancer trap line, *rP668*, with a P element inserted in the 73C1-2 double band, where *nrt* maps, was subsequently shown to be an *nrt* mutant allele (*nrt*^{rP668}). In this allele, Nrt appears to be absent from the embryonic and pupal PNS (data not shown) and its accumulation in the CNS is reduced (Figures 1C and 1G). The P insertion site in *nrt*^{rP668} was mapped by Southern blot analysis and PCR to the transcribed region of *nrt*, at 438 bp before the translation start site (Figure 2A; de la Escalera et al., 1990). Despite this, a probe specific to the 5′ untranslated leader sequence common to the three *nrt* mRNAs (de la Escalera et al., 1990; Hortsch et al., 1990b) hybridized in situ to the CNS of *nrt*^{rP668} embryos (data not shown), albeit producing a weaker signal than normal. This indicates that transcription in the mutant CNS still initiates at a position(s) 5′ to the translation start site and that a normal protein

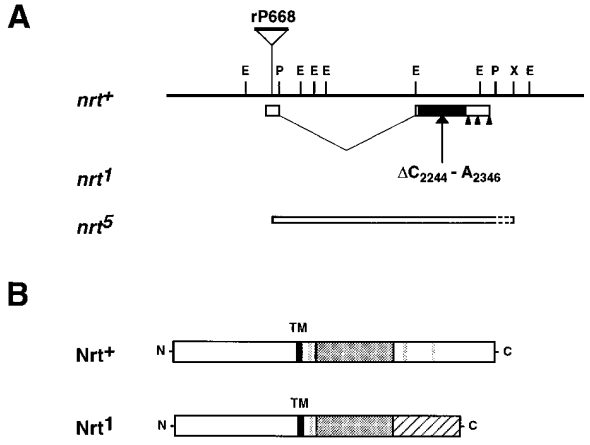

Figure 2. Structure of the *nrt* Gene in Wild-Type and Mutant Alleles

(A) Restriction map of cloned genomic DNA surrounding the *nrt* transcription unit. All EcoRI (E), but only two PstI (P) sites and one Xho (X) site, are depicted. The insertion site of the P element in the strain *rP668* is shown. Below, the transcription unit is shown by a bar, with the closed region representing the coding sequence. The gene contains a single large intron, although introns smaller than 20–30 bp would have passed undetected in our analysis. Three polyadenylation sites are indicated by arrowheads. The position of the small deletion in nrt^1 is shown (nucleotide numbers according to de la Escalera et al., 1990), as well as the extent of the nrt^5 deletion.

(B) Schematic diagram of the Nrt protein. The transmembrane domain (TM; closed box) and the region of higher sequence homology to serine esterases in the extracellular domain (amino acids 380–580; stippled box; de la Escalera et al., 1990) are indicated. Stippled bars represent the LRE tripeptide which is the primary sequence of the adhesive site of s-laminin (Hunter et al., 1989). The deletion in nrt^1 introduces a frameshift that results in an unrelated amino acid sequence (hatched box) after amino acid position 580 in the extracellular C terminus of the mutant protein.

can be made. Nevertheless, the insertion probably blocks the action of an enhancer(s) that drives Nrt expression in the PNS. Therefore, nrt^{rP668} is apparently a hypomorphic mutation in the CNS and a null mutation in the PNS.

Excision lines of the P-insertion in nrt^{rP668} were generated, and those carrying deletions of adjacent *nrt* sequences were detected by staining with mAb 43B5. Some were analyzed molecularly as well. One excision strain, nrt^5, is a null mutation, most likely of a single gene, since it deletes the *nrt* transcribed region only (Figure 2A). Although nrt^5 completely abolishes Nrt expression (Figure 1D), flies of this genotype are viable and fertile.

neurotactin Mutations Cause Defasciculation of the Ocellar Pioneer Nerve

We analyzed Nrt requirements in the adult dorsal head, where different neighbor neurons select alternative substrates for axon projection (García-Alonso et al., 1996). During early pupal development, ocellar pioneer axons extend in the extracellular matrix (ECM) that cover the internal side of the prospective head without contacting the epithelium (Figure 3A). After head eversion, the ocellar pioneer nerve becomes displaced to its final position perpendicular to the epidermal surface and the brain (see scheme in Figure 3F; for a full description of ocellar nerve development see García-Alonso et al., 1996). Mechanoreceptor neurons from Ocellar and Orbital bristles also start extending their axons before head eversion; however, they seem to follow epithelial cues toward their targets in the brain and remain associated with the epidermis once head eversion has taken place (Figure 3D). Recognition of these two different substrates (ECM versus epidermis) by the growth cones and the choice to attach or not to the epidermis is vital for both types of axons to project to their correct targets after head eversion (García-Alonso et al., 1996). In order to be displaced perpendicular to the epidermis and the brain after head eversion, ocellar pioneer axons must not adhere to the epidermis. Conversely, mechanoreceptor axons should be associated with the epidermis in order to continue following this surface after head eversion. Therefore, ocellar pioneer axons should recognize and be guided by a different subset of cues than mechanoreceptors.

Nrt is expressed by all ocellar pioneer neurons from the onset of axon extension, but it is not expressed by mechanosensory neurons (Figure 3B). Mutations in *nrt* frequently cause defasciculation of the normally tightly associated ocellar pioneer axons (Figure 3C; Table 1). Before head eversion in mutant pupae, this phenotype is predominant, but the penetrance decreases after head eversion (data not shown), possibly due to the new association of glial cells with the ocellar pioneer nerve and the subsequent enwrapping of the four fascicles by two sheets of glia (García-Alonso et al., 1996). The defasciculation phenotype must result from a specific requirement for Nrt, since in *R20F*, an excision revertant chromosome of the P insertion in nrt^{rP668} that apparently restores normal Nrt expression, these phenotypes are strongly reduced (Table 1). Despite this frequent defasciculation phenotype, ocellar pioneer axons usually reach their brain targets. Occasionally, ocellar pioneer axons associate with the epidermis and remain attached to it, sometimes stalling or connecting with the neighbor mechanoreceptor axons and following them for some distance along the epidermal contour (Figure 3E). This latter phenotype suggests a role (direct or indirect) of Nrt for ocellar pioneer growth cone guidance. We never observed bristle axons detaching from the epidermal surface or connecting with the ocellar pioneer nerve in *nrt* mutants, conditions that would have revealed that the mechanoreceptor axons had chosen their alternative substrate for extension (see below).

Neurotactin Can Function as an Instructive Guidance Cue for Adult Sensory Neurons

Gain-of-function phenotypes produced by ectopic gene expression are another way to reveal function (reviewed by Goodman, 1996). To this aim, we used the GAL4 system (Brand and Perrimon, 1993) to direct altered patterns of Nrt expression in a genetic background devoid of the normal Nrt expression. In pupae of the genotype $GAL4^{Mz1407}$ *UAS–nrt*/*UAS–nrt*; nrt^5 stained with mAb 43B5, a small fraction of ocellar pioneer and many (but not all) mechanoreceptor axons showed Nrt accumulation (data not shown). Accordingly, the defasciculation

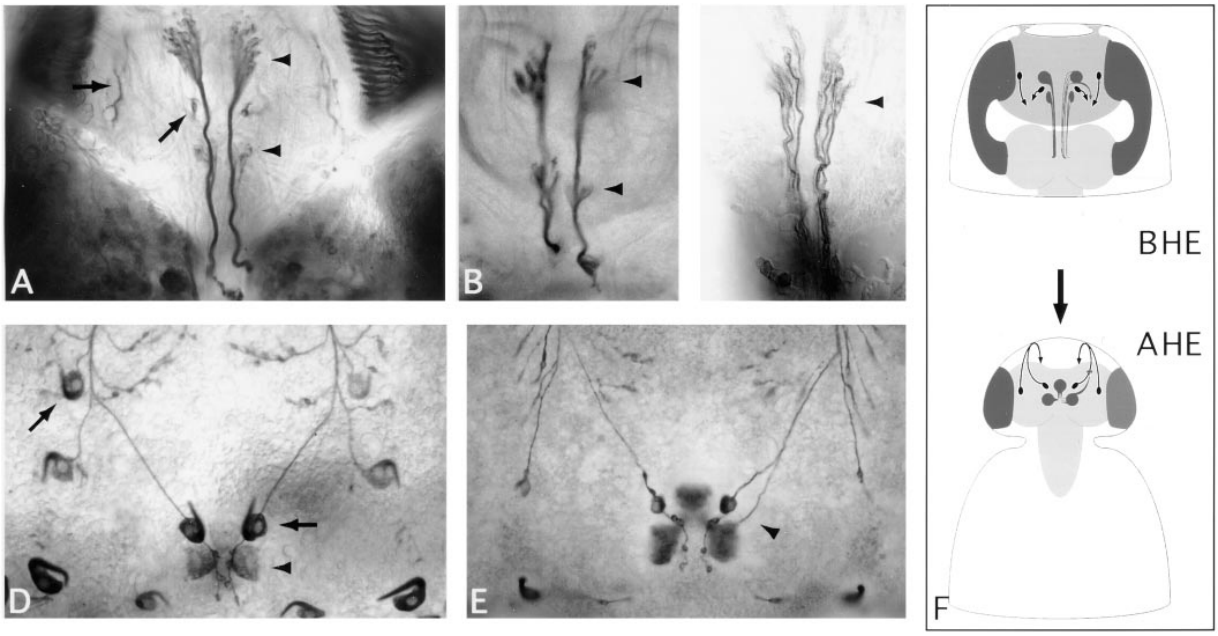

Figure 3. Neurotactin Is Required by Ocellar Pioneer Axons for Fasciculation and Pathfinding

(A) In the wild-type pupa before head eversion, ocellar pioneer axons (arrowheads) project in the ECM. The ~50 axons from each ocellus extend straight in parallel and completely fasciculated to each other up to the brain (bottom of image). Axons of the bristle neurons (arrows) project in the epidermis in the neighborhood of ocelli, but with a meandering trajectory, toward a different target in the brain.

(B) Ocellar pioneers from a wild-type individual show expression of Nrt.

(C) Example of an extreme ocellar pioneer axon defasciculation phenotype in nrt^5, similar to that found in other *nrt* mutations.

(D) The early wild-type pupal configuration of ocellar pioneer and mechanoreceptor axons (A) changes dramatically after head eversion; when the head capsule evaginates, the brain comes to lie within it and the ocellar pioneer nerve becomes displaced to its final position perpendicular to the dorsal surface of the head. Bristle axons (arrows) remain attached to the epidermis.

(E) In *nrt* mutations, as in the nrt^{rP668} pupa shown here, some ocellar pioneer axons (arrowheads) may attach to the epidermis.

(F) The scheme shows the general aspect of head and thorax (wings have been omitted for simplification) at two pupal stages, before head eversion (BHE, as in [A] through [C]) and after head eversion (AHE, as in [D] through [E]). Left sides summarize wild-type patterns of axon projection of ocellar pioneer neurons, Orbital (only one is depicted for simplification), and Ocellar bristle neurons. Right sides summarize *nrt* loss-of-function phenotypes.

(A and C–E), mAb 22C10; (B), mAb 43B5.

phenotype of the ocellar pioneer nerve in nrt^5 was not corrected (Table 1). Nevertheless, in 21 of 42 pupal heads (50%) after head eversion, axons of mechanoreceptors (Ocellar and Postvertical) leave the epidermal surface and associate with the ocellar pioneer nerve (Figure 4E). These bristle axons start projection at their normal cell site but soon after initial extension turn toward the ocellar pioneers and contact them (see Figures 4D and 4E). To improve Nrt expression, we used the insertion $GAL4^{G537.4}$ in the gene *scabrous* (Hinz et al., 1994). Before head eversion, pupae of the genotype $GAL4^{G537.4}/GAL4^{Mz1407}$ *UAS–nrt*; nrt^5 showed Nrt accumulation in most or all ocellar pioneer axons and in large patches of epithelial cells around the location of ocelli and mechanoreceptors (Figure 4A). Three classes of phenotypes were found in these pupae. After head eversion, 12 of 17 pupal heads (70%) were like those just described, with mechanoreceptor axons projecting away from the epidermis in association with the ocellar pioneers (Figure 4D). Also after head eversion, 9 of 17 pupal heads (53%) had ocellar pioneer axons projecting into the epidermis that either stalled or extended for some distance following the mechanoreceptor axons (Figures 4B and 4F). Finally, 12 of 77 pupal heads (16%) before eversion had an epidermal phenotype in which both sides of the head capsule came closer together due to a fold along the midline of the head (Figure 4C). This phenotype correlates with the epithelial expression of Nrt at both sides of the head midline. In this genetic combination, ocellar pioneer axons seem to fasciculate

Table 1. Defasciculation Phenotype of Ocellar Pioneer Axons before Head Eversion in Loss- and Gain-of-Function Conditions for *nrt*

Genotype	Penetrance[a]
nrt^1	10/12 (83%)
nrt^5	7/10 (70%)
nrt^1/nrt^5	24/36 (66%)
$nrt^1/Df(3L)st^{81k17.2}$	5/6 (83%)
nrt^{rP668}	6/12 (50%)
R20F	3/27 (11%)
$GAL4^{Mz1407}$ *UAS–nrt/UAS–nrt*; nrt^5	37/52 (71%)
$GAL4^{G537.4}/GAL4^{Mz1407}$ *UAS–nrt*; nrt^5	20/77 (26%)[b]

[a] Presence of any single split within the ocellar pioneer fascicles was considered to be defasciculation.

[b] This number represents a maximum, since defasciculation within the ECM could not be distinguished from splitting of the fascicle caused by the adhesion and extension of the ocellar pioneer axons along the epidermis before head eversion.

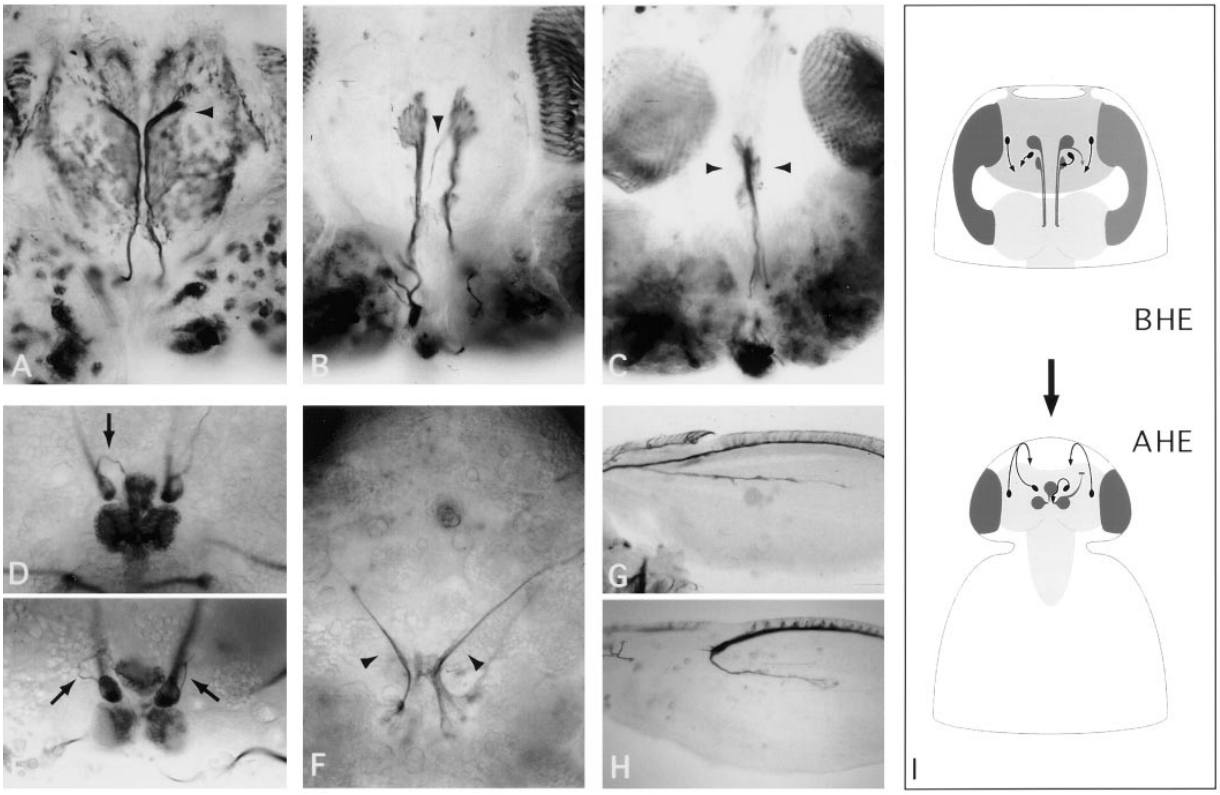

Figure 4. Neurotactin Displays a Capacity as an Instructive Guidance Cue

(A) Expression of Nrt in *GAL4*$^{G537.4}$/*GAL4*^{Mz1407} *UAS–nrt*; *nrt*^{5} pupal head capsule before head eversion. In addition to expression in ocellar pioneers (arrowhead), there is expression in large patches around ocellar pioneers and bristles.

(B) Some ocellar pioneer axons project in the epidermis in these pupae (arrowhead) and stall.

(C) Some other pupae of this genetic constitution display a fold along the head midline between both fascicles from left and right ocellar pioneers (arrowheads); the fold brings left and right sides closer together.

(D) *GAL4*$^{G537.4}$/*GAL4*^{Mz1407} *UAS–nrt*; *nrt*^{5} pupae after head eversion show bristle axons (Ocellar or Postvertical) projecting to the ocellar pioneer nerve. In this case, one Ocellar bristle axon (arrow) is projecting with the ocellar pioneers, while the other is extending normally (note that the cell polarity of the neuron is normal but the axon turns toward the ocellar pioneer cell bodies soon after its birth).

(E) A similar phenotype is shown by pupae of the genotype *GAL4*^{Mz1407} *UAS–nrt*/*UAS–nrt*; *nrt*^{5}. In this case, both Ocellar bristle axons (arrows) are projecting to the medial ocellus.

(F) *GAL4*$^{G537.4}$/*GAL4*^{Mz1407} *UAS–nrt*; *nrt*^{5} pupae display ocellar pioneer axons (arrowheads) projecting in the epidermis after head eversion.

(G) In the wild type, axons from the triple row and the third vein sensilla converge projecting out of the wing toward the CNS.

(H) In *GAL4*$^{G537.4}$/*GAL4*^{Mz1407} *UAS–nrt; nrt*^{5} pupae, axons from the triple row may not extend out of the wing, and third vein sensilla axons connect with them in a loop.

(I) The scheme shows the general aspect of head and thorax (wings have been omitted for simplification) at two pupal stages, before head eversion (BHE, as in [A] through [C]) and after head eversion (AHE, as in [D] through [H]). Left sides summarize wild-type patterns of axon projection of ocellar pioneer neurons, Orbital (only one is depicted for simplification), and Ocellar bristle neurons. Right sides summarize *nrt* gain-of-function phenotypes.

(A), mAb 43B5; (B–H), mAb 22C10.

much better than in the *nrt*^{5} mutant (Table 1); however, the fact that some ocellar pioneer axons attach to the epithelial surface makes the presence of some splitting in the nerve inevitable.

Neurons of the triple row in the anterior margin of the wing, but not sensillum neurons in the third vein, express Nrt in wild type (data not shown). No obvious phenotype in the axon-extension pattern of wing neurons is found in *nrt*^{5} pupae. However, *GAL4*^{Mz1407} *UAS–nrt*/*UAS–nrt*; *nrt*^{5} and even more *GAL4*$^{G537.4}$/*GAL4*^{Mz1407} *UAS–nrt*; *nrt*^{5} pupae, which ectopically express Nrt in all wing neurons as well as in veins I and III, do show a mutant phenotype. Frequently, vein III sensilla have axons that turn back toward axons of the triple row, creating a loop that prevents both types of axons from leaving the wing in the direction of the CNS (compare Figures 4G and 4H). In addition, analysis of the projection patterns of bristle axons of the pupal notum also reveals errors in their extension. For example, axons from Scutellar bristles can erroneously project to the contralateral side or even into the abdomen (data not shown). These results are consistent with the idea that Nrt has the capacity to provide axons with guidance cues.

The Embryonic CNS Phenotype of *neurotactin* Mutants

Despite its extensive expression in the embryo, Nrt is not essential for fly development. Accordingly, staining

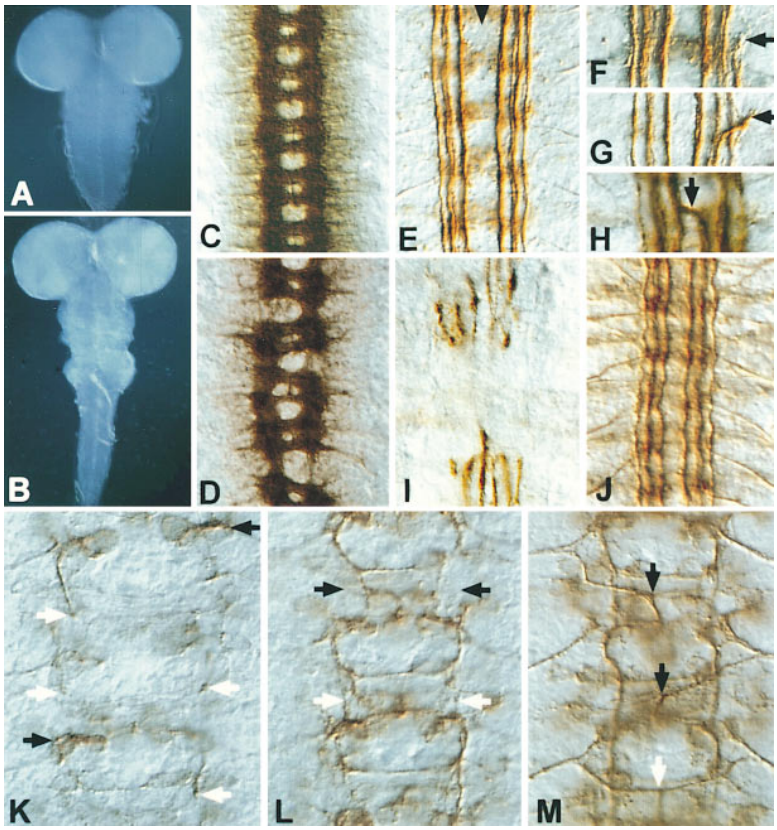

Figure 5. The Embryonic CNS Phenotype of Single *nrt*^{5} and Double *nrg*^{1}; *nrt*^{5} Mutants

(A) CNS of a late third instar wild-type larva.
(B) CNS of a late third instar *nrt*^{5} larva.
(C) Axonal scaffold of a wild-type embryo stained with mAb BP102.
(D) Defective axonal scaffold of a *nrg*^{1}; *nrt*^{5} embryo stained with mAb BP102.
(E–H) Portion of a wild-type CNS stained with mAb 1D4, showing the three main Fas II axon bundles at both sides of the midline (arrowhead, [E]). In an *nrt*^{5} embryo, Fas II axons may stall (arrow in [F]) or be misrouted and subsequently stall (arrow in [G]) or cross the midline and fasciculate with other Fas II axons (arrow in [H]).
(I and J) Severe defects are observed in the Fas II axonal pattern of a *nrg*^{1}; *nrt*^{5} embryo (I). This mutant phenotype is rescued by expression of a *UAS–nrt* transgene driven by line *GAL4*^{Mz1277}, as shown in (J).
(K–M) Specific defects in *nrg*^{1}; *nrt*^{5} embryos are also detected with mAb 22C10.
(K) Early in axogenesis, dMP2 axons may grow normally (white arrows mark the position of the growth cones) or stall (black arrows).
(L) Later, the MP1 fascicle (white arrows mark normal axons) may be absent in some hemisegments (black arrows).
(M) The axon fascicle of the six midline VUM neurons projects dorsally and then normally splits in two branches (white arrow), which project at either side of the midline. The splitting does not occur in some mutant segments (black arrows).

of *nrt*^{5} embryos with mAb BP102 (Seeger et al., 1993), which marks all CNS axons, did not reveal gross defects (data not shown). However, a slightly delayed axogenesis, a lack of nerve cord condensation that persisted postembryonically (compare Figures 5A and 5B), and a mild constriction of the nerve cord at a random location were observed consistently in *nrt*^{5} embryos. These defects may be attributed to a reduction in adhesiveness among neural cells. Staining with mAb 1D4 to label Fas II-expressing axons (Grenningloh et al., 1991) uncovered subtle but distinct defects of Fas II axons, both in homozygous and transheterozygous embryos carrying the alleles *nrt*^{1} and *nrt*^{5}. These defects were not observed in *nrt*^{rP668} embryos, the line from which *nrt*^{5} is derived (Table 2, lines 1–4). The defects were observed in 10%–15% of hemisegments, and consisted mainly of stalling or misrouting and subsequent stalling of axons; rarely did misrouted axons cross the midline (Figures 5F–5H). These phenotypes were observed in *nrt* alleles with a different genetic background, indicating a partial requirement of Nrt for axon outgrowth and growth cone guidance in the CNS. They also suggest that *nrt*^{1} is a strong hypomorph or even a null allele like *nrt*^{5}.

The Embryonic CNS of Double Mutants for *neurotactin* and Other Genes Encoding Neural CAMs: a Synergistic Interaction between *neurotactin* and *neuroglian*

The lack of widespread axonal defects in the CNS of *nrt* mutants suggests that the function of Nrt in CNS morphogenesis might be largely replaced by functionally related molecules. If so, embryos lacking both Nrt and one of these other molecules may display synergistic mutant phenotypes. To test this possibility, we analyzed embryos lacking function of both *nrt* and one of several genes encoding neural CAMs.

Nrg is a *Drosophila* neural CAM related to several vertebrate CAMs, though most closely to mouse L1 (Bieber et al., 1989). Two forms of Nrg that differ in their cytoplasmic domains and patterns of expression are known (Hortsch et al., 1990a). The long Nrg isoform is neural-specific; it is initially (early stage 12) found in a fraction of CNS neurons (Hortsch et al., 1990a), but during stage 13 it can be detected in most (and probably all) differentiating neurons (data not shown). The short Nrg isoform is expressed by glia, is widely expressed in other tissues, and is probably expressed throughout the entire CNS (Hortsch et al., 1990a). *nrg*^{1}, a loss-of-function mutation for both Nrg forms, is lethal and causes motor neuron pathfinding defects, but the overall CNS structure of mutant embryos looks normal (Bieber et al., 1989; Hall and Bieber, 1997). Furthermore, unlike *nrt*^{5} embryos, no defects were detected with mAb 1D4 in *nrg*^{1} embryos (Table 2, line 5). In contrast, *nrg*^{1}; *nrt*^{5} double mutant embryos have a severe CNS phenotype. With mAb BP102, we observed thinning or complete interruption of longitudinal connectives, as well as fusion of commissures (compare Figures 5C and 5D). Fas II fascicles exhibit similar abnormalities to those observed in *nrt*^{5} embryos, albeit with a much higher expressivity

Table 2. The Phenotype of Fasciclin II-Expressing Axons at Stage 16 in *nrt*, *nrg*; *nrt*, and *kek1*; *nrt* Mutant Embryos

Genotype	Affected Hemisegments (%)[a]		
	Stalling	Misprojection	Total
nrt^{rP668}	1	<1	
nrt^{1}	4	11	
nrt^{5}	6	6	
nrt^{1}/nrt^{5}	5	8	
nrg^{1}	<1	0	
nrg^{1}; nrt^{P668}	9	5	
nrg^{1}; nrt^{rP668}/nrt^{5}	26	19	
nrg^{1}; *R20F*	1	2	
nrg^{1}; nrt^{5}			79
nrg^{1}; nrt^{1}/nrt^{5}			84
nrg^{1}; nrt^{5}/*Df(3L)std11*			94
nrg^{2}; nrt^{5}			38
nrg^{2}; nrt^{1}			38
nrg^{2}; nrt^{1}/nrt^{5}			33
$kek1^{RM2}$	<1	2	
$kek1^{RM2}$; nrt^{5}	28	32	

[a] The mild defects found in embryos of genotypes 1–8, 15, and 16 were allowed to distinguish between stalling and misprojection phenotypes, even though both might be present in a same hemisegment. The severe defects of genotypes 9–14 were allowed only to record the total number of affected hemisegments. More than 100 hemisegments were examined in each case.

and penetrance. Most notably, interruptions of the longitudinal axon bundles were frequent, as were misguidance phenotypes (Figure 5I; Table 2, line 9). Double mutant embryos, like single nrt^{-} embryos, also showed a local constriction of the ventral nerve cord with a variable expressivity. This defect may be a consequence of the impaired axogenesis and condensation of the nerve cord. No defects outside the CNS were evident in the double mutants.

Using mAb 22C10, which recognizes a subset of neurons (Fujita et al., 1982; Goodman et al., 1984), and mAb 1D4, we analyzed the behavior of several identified pioneer axons during early stages of axogenesis in nrg^{1}; nrt^{5} embryos (Figures 5K–5M). We observed that the pioneer axon of the intersegmental nerve, aCC, as well as the pioneer axon of the segmental nerve, establish their correct pathways. Likewise, the axons of the U neurons follow the aCC pathway correctly. In contrast, in 37 of 128 cases (29%), the axons of the dMP2 and MP1 neurons, pioneers of the MP1 pathway, do not normally defasciculate from the aCC axon to turn posteriorly, but either stall or delay their extension considerably (Figures 5K and 5L). Other axons showing misguidance phenotypes are those of the six ventral unpaired medial (VUM) neurons. In the wild type, the VUM axons initially fasciculate together before splitting into two fascicles that grow laterally at either side of the midline, passing the RP2 neuron and fasciculating with the corresponding anterior aCC axon (Figure 5M; Klämbt et al., 1991; Bossing and Technau, 1994). In 19 of 128 (15%) double mutant segments, the fascicle of VUM axons either does not split or splits into more than two fascicles, each joining a different aCC axon, including that of the same hemisegment (Figure 5M). The first two axons of the vMP2 pathway, pCC (the pioneer) and vMP2, grow correctly in most hemisegments; only in 4 of 128 cases did we observe a misrouted vMP2 axon. Anomalies in the trajectory of the SP1 axon were also observed, though rarely. nrg^{1}; nrt^{5} embryos also displayed, due to slight mispositioning of cells, a somewhat irregular appearance of what is normally a highly stereotyped pattern of neurons (Figures 5K–5M). However, relative positions of neurons were maintained.

It seems most likely that the phenotypes of nrg^{1}; nrt^{5} embryos result from a direct requirement for these two CAMs during axogenesis, and not as a secondary consequence of a previous requirement during neurogenesis. Thus, expression of the nuclear proteins Eve, Ftz, and En, markers of the specification of subsets of neurons that are arranged in characteristic patterns (Doe et al., 1988a, 1988b; Patel et al., 1989), was found to be normal in nrg^{1}; nrt^{5} embryos between stages 12 and 16 (data not shown). This suggests that a failure of proper cell fate determination does not cause the axonal mutant phenotype. Likewise, glial cells expressing Repo, a specific marker for most of the CNS glia (Halter et al., 1995), form at the correct time and place and in normal number in nrg^{1}; nrt^{5} embryos. The longitudinal glia (LG), which could provide a matrix for longitudinal axon extension (Jacobs and Goodman, 1989; Jacobs et al., 1989), migrate and arrange normally in the double mutant, prefiguring the longitudinal connectives. It is from stage 14 onward, when the LG normally stretch in the anterior-posterior direction and enwrap the connectives, that gaps in the LG begin to appear, overlapping with gaps in the connectives (data not shown). It is most likely, therefore, that this LG phenotype in late mutant embryos is a consequence, rather than the origin, of the interruptions observed along the axonal connectives.

The interaction between *nrg* and *nrt* is gene-specific and is not attributable to the particular genetic background of any of the alleles employed. Thus, phenotypes similar to those of nrg^{1}; nrt^{5} embryos are also found in embryos carrying nrg^{1} and nrt^{5} over other strong alleles of independent origin such as nrt^{1} or *Df(3L)std11* (Table 2, lines 10–11). Also, double mutants involving nrt^{rP668}, which does not display a mutant phenotype by itself, show mild but consistent mutant phenotypes (Table 2, lines 6–7). Yet embryos of the genotype nrg^{1}; *R20F* (*R20F* serves as a wild-type control for the genetic background of nrt^{rP668} and nrt^{5}) are essentially normal (Table 2, line 8). Also, the partial loss-of-function mutation nrg^{2} (Bieber et al., 1989; Hall and Bieber, 1997) combined with strong *nrt* alleles yielded similar phenotypes (Table 2, lines 12–14), but with a lower expressivity and penetrance than in the combinations involving nrg^{1}.

Finally, targeted neural expression of Nrt during axogenesis was driven in the nrg^{1}; nrt^{5} background with the GAL4 system (Brand and Perrimon, 1993), to attempt the rescue of the mutant phenotype (see Experimental Procedures). With the use of line $GAL4^{Mz1277}$ and a *UAS–nrt* transgene, high levels of Nrt expression could be specifically restored in all CNS and a few PNS neurons of nrt^{5} embryos (Figure 1H). This GAL4-driven expression started at early stage 12 when postmitotic neurons begin to differentiate. Embryos of the genotype nrg^{1}; *UAS–nrt*/+; $GAL4^{Mz1277}$ nrt^{5}/nrt^{5} were found to display a normal axonal pattern (Figure 5J). Therefore, we conclude that the absence of Nrt in central neurons during axogenesis

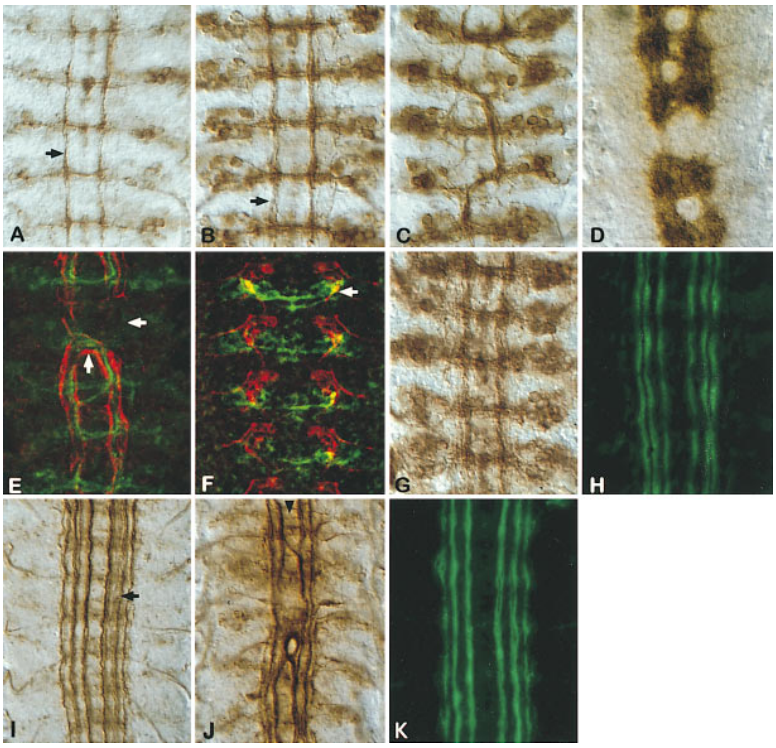

Figure 6. The Embryonic CNS Phenotype of *drl*$^{P3.765}$; *nrt*^{5} and *kek1*^{RM2}; *nrt*^{5} Double Mutants

(A) Anti-β-gal staining of a *drl*$^{P3.765}$/+ embryo focused at the level of the Drl-expressing DV axon bundle (arrow).

(B) In the homozygous *drl*$^{P3.765}$ embryo shown here, some defasciculation can be noticed in a DV bundle (arrow). Staining is stronger than in (A) due to the homozygosity of the P insertion.

(C) Strong defects in the Drl axonal pattern are evident in a double *drl*$^{P3.765}$; *nrt*^{5} embryo.

(D) The axonal defects in *drl*$^{P3.765}$; *nrt*^{5} mutants extend to many other axons, as revealed by the general axonal marker mAb BP102.

(E) Confocal image of a *drl*$^{P3.765}$; *nrt*^{5} embryo at stage 16 double stained to show Drl (anti-β-gal antibody; green) and Fas II (mAb 1D4; red) fascicles. Note defects of Fas II fascicles associated to defects of Drl fascicles (arrows).

(F) In a stage 13 *drl*$^{P3.765}$/+ embryo, stained as in (E), growing dMP2 axons which express Fas II appear to contact Drl-expressing neurons (arrow).

(G–H) In the same *UAS–nrt drl*$^{P3.765}$/*drl*$^{P3.765}$; *GAL4*^{Mz1277} *nrt*^{5}/*nrt*^{5} embryo, normal projection patterns of both Drl (G) and Fas II (H) axons are rescued.

(I) Some defasciculation of Fas II axon bundles can be detected in a single *kek1*^{RM2} embryo (arrow), but the projection pattern is normal.

(J) In a double *kek1*^{RM2}; *nrt*^{5} embryo, strong defects of the Fas II axonal pattern are evident.

(K) Rescue of the Fas II axonal phenotype in a *UAS–nrt kek1*^{RA5}/*kek1*^{RM2}; *GAL4*^{Mz1277} *nrt*^{5}/*nrt*^{5} embryo.

is the cause of the CNS mutant phenotype in *nrg*^{1}; *nrt*^{5} embryos.

We analyzed combinations of *nrt*^{5} with null mutations in five other CAM genes: *FasI*, *FasII*, *FasIII*, *plx*, and *nrm*. All of these genes display more restricted CNS expression patterns than *nrg* or *nrt*. With the exception of *nrm* (Kania and Bellen, 1995), their loss-of-function condition produced no visible phenotype in the CNS when viewed under the light microscope. Using various antibody probes (see Experimental Procedures), we did not detect synergistic phenotypes in any of the double mutants.

Phenotypic Interactions of *neurotactin* with *derailed* and *kekkon1*

Several other membrane-bound molecules for which a CAM function has not yet been formally demonstrated have also been implicated in axon guidance. Following the same rationale as above, we analyzed embryos double mutant for *nrt* and each one of the following genes: *drl*, *kekkon1* (*kek1*), *Ptp69D*, and *Ptp99A*.

The *drl* gene encodes a receptor tyrosine kinase required by a subset of interneurons to make correct axonal pathway choices (Callahan et al., 1995). The mutant allele *drl*$^{P3.765}$ has an inserted P[*etau-lacZ*] element which can be used to reveal Drl^{-} expressing neurons and their axons (Callahan et al., 1995). Drl axons project contralaterally across the anterior commissure and then turn anteriorly forming two fascicles, termed DD and DV (Figure 6A). Within the CNS, homozygous *drl*$^{P3.765}$ mutants displayed partial defasciculation of Drl axon bundles, but their projection patterns are essentially normal (Callahan et al., 1995; Figure 6B). In *drl*$^{P3.765}$/+; *nrt*^{5} embryos, Drl fascicles look normal (data not shown). In contrast, all *drl*$^{P3.765}$; *nrt*^{5} and *drl*$^{P3.765}$/*Df(2L)TW130*; *nrt*^{5} embryos examined showed strong misguidance and stalling phenotypes of Drl axons in many segments (Figure 6C). Interestingly, mAbs BP102 (Figure 6D) and 1D4 (Figure 6E) in both double mutant combinations show that many axons that do not normally express Drl display similar defects to those exhibited by Drl axons. This reveals a nonautonomous requirement of Drl in those axons. Although at stage 16 Drl and Fas II axon bundles do not appear to contact each other (Figure 6E), we observed that at mid-stage 13, the extending axon of dMP2, a Fas II-expressing neuron, appears to contact Drl neurons (Figure 6F). The *drl* mutant alleles used here have an independent origin, strongly suggesting that it is the lack of drl that contributes to the phenotype of the double mutants. On the other hand, GAL4-driven Nrt expression in differentiating CNS neurons of double *drl*$^{-}$ *nrt*$^{-}$ embryos (i.e., in embryos of the genotype *UAS–nrt drl*$^{P3.765}$/*drl*$^{P3.765}$; *GAL4*^{Mz1277} *nrt*^{5}/*nrt*^{5}) was able to restore the normal projection patterns of both Drl and Fas II fascicles (Figures 6G and 6H). This result confirms that the double mutant phenotype is produced by the specific lack of Nrt in the CNS during axogenesis.

kek1 (Musacchio and Perrimon, 1996) is one of two closely related genes that encode transmembrane proteins with structural homology to CAMs and signaling molecules. The gene is expressed in many CNS neurons and midline cells during axogenesis. No major abnormalities were observed in the CNS of *kek1* mutant embryos (Musacchio and Perrimon, 1996; Table 2, line 15),

although partial defasciculation of Fas II axon bundles can be sometimes detected in *kek1^{RM2}* embryos (Figure 6I). In *kek1^{RM2}*; *nrt^{5}* as well as in *kek1^{RM2}*/*kek1^{RA5}*; *nrt^{5}* embryos stained with mAb BP102, extension of longitudinal axons through the intercommissural region is frequently affected (data not shown). Also, a complex phenotype is detected with mAb 1D4: Fas II axons display defasciculation, stalling, and guidance defects in all double mutant embryos examined (Figure 6J; Table 2, line 16). Most notably, Fas II axons frequently cross the midline, a phenomenon rarely observed in *nrt^{5}* embryos. These defects are indeed due to the absence of Nrt in differentiating neural cells, since the axon stalling and misguidance phenotypes could be rescued in embryos of the genotype *UAS–nrt kek1^{RA5}*/*kek1^{RM2}*;*GAL4^{Mz1277} nrt^{5}*/*nrt^{5}* (Figure 6K).

Ptp69D and *Ptp99A* each encode a CAM-like receptor tyrosine phosphatase which, like Nrg, is selectively expressed in most or all CNS axons (Tian et al., 1991; Yang et al., 1991). Single gene mutations in *Ptp69D* or *Ptp99A* do not affect the overall morphology of the CNS, although perturbation of motor axon guidance once these axons leave the ventral nerve cord has been reported (Desai et al., 1996, 1997). In contrast to *nrg* mutants, the CNS phenotype of double mutant *Ptp69D^{1} nrt^{5}*/*Df(3L)8ex25 nrt^{5}* (which carry two nonoverlapping deletions of *Ptp69D*; Desai et al., 1997) and *Ptp99A^{1} nrt^{5}* embryos does not differ significantly from that of single gene *nrt^{5}* embryos (data not shown).

Discussion

The Function of Neurotactin in Axogenesis

Previous studies indicated that Nrt is able to mediate cell adhesion in cell culture (Barthalay et al., 1990; Hortsch et al., 1990b; Darboux et al., 1996). The mutational analysis presented here shows that the in vivo function of Nrt is consistent with the characteristics of a neural CAM involved in axogenesis.

The role of several other CAMs in neural development has already been tested by genetic means using lack-of-function mutants or conditions of ectopic gene expression (i.e., gain-of-function situation), both in *Drosophila* and in vertebrates. Mild phenotypes are a rather common theme in loss-of-function conditions of neural CAM genes. Thus, in *Drosophila* embryos lacking *nrg*, the overall structure of the CNS develops normally (Bieber et al., 1989); in this case, only motor neuron pathfinding defects have been detected (Hall and Bieber, 1997). Altered presynaptic function and uncoordinated adult behavior (*FasI^{-}*; Zhong and Shanley, 1995) or selective defasciculation only observed at the EM level (*FasII^{-}*; Lin et al., 1994) are other examples of subtle mutant phenotypes. In the case of *nrt*, mutant phenotypes affecting axonal outgrowth, fasciculation, and guidance are also mild in most instances.

The most consistent axonal phenotype in *nrt* null individuals is defasciculation of the ocellar pioneer nerve. It is clear, however, that Nrt is not the only molecule implicated in ocellar pioneer nerve fasciculation: although the penetrance of ocellar pioneer axon defasciculation is high, expressivity is far from complete and many axons remain fasciculated. In contrast, a similar defasciculation phenotype is not evident in the CNS of *nrt* null embryos, perhaps because it is difficult to reveal, as it was in the case of *FasII* null mutants (Lin et al., 1994). The apparent lack of defasciculation phenotypes in the CNS might result from redundant adhesion pathways, which may exist in larger number in the CNS than in the ocellar pioneer nerve. It is not unreasonable to speculate that additional constraints might be imposed by the high axonal and cell body density in contrast to the unrestrained navigation of ocellar pioneer axons in the ECM. In *nrt* null mutants, some ocellar pioneer axons can project in the epidermis, but there they eventually stall. This phenotype suggests either that the epidermis inhibits ocellar axon extension (through an active signaling process or a purely mechanical constraint) or that the molecules involved in the interaction of ocellar pioneer growth cones with the epidermal cell surface are not able to produce the signals necessary to maintain ocellar axon extension. Nevertheless, ectopic expression of Nrt in the epidermal cell surface can produce exactly the same phenotype, indicating that ocellar pioneer growth cones recognize and interact with Nrt in the epidermal cells. This last result strongly suggests that the epidermis inhibits ocellar pioneer axon extension. The molecules involved in this inhibition, however, must not operate over mechanoreceptor growth cones.

The stalling phenotype of CNS axons in *nrt* null embryos could reflect a role of Nrt in promoting axon outgrowth, or it could be a consequence of an altered selection of substrate as in the case of ocellar pioneers. The misrouting phenotypes also suggest that Nrt may function, directly or indirectly, as a guidance cue. A likely requisite for a molecule to carry out a guidance function is that it ought to be unequally distributed within the neural population. Nrt might partially fulfill this requirement since, despite its broad expression in the CNS, it seems to accumulate unevenly in different neural cells. Likewise, the misrouting of sensory axons under ectopic expression of Nrt might indicate that it can indeed function as a guidance molecule. Nevertheless, pathfinding phenotypes in loss-of-function conditions could also reflect a generic requirement of Nrt for fasciculation to stabilize growth and recognition along specific pathways. Selective fasciculation is a mechanism of growth cone guidance experimentally distinguishable from directional guidance (Lin et al., 1994). In the case of the ocellar pioneer axon guidance, however, fasciculation is revealed as a mechanism that can subserve directional guidance. Thus, fasciculation mediated by Nrt, as in the ocellar pioneer nerve, could serve as a mechanism to integrate the guidance of individual growth cones by CAMs and related molecules of more restricted expression, in order to generate robust and precise pathfinding toward the correct targets. This could be necessary if individual growth cone guidance is not an accurate process. In the course of such cooperative function, the weakening of adhesion between the ocellar pioneer axons would make them prone to errors such as projecting to an alternative substrate (the epidermis). This could explain why an ocellus has so many pioneer neurons ($\sim$50). Fasciculation of ocellar pioneer axons can then be understood as a mechanism subserving directional guidance. In this regard, it should be noted that

the PNS expression of Nrt is prominent in polyinnervated sensory organs including ocelli and eye ommatidia neurons, the axons of which grow together toward the CNS.

It has been suggested recently that Nrt can mediate homotypic cell adhesion through a secreted molecule acting as an intermediate ligand (Darboux et al., 1996). The phenotypes reported here for loss-of-function conditions and ectopic Nrt expression are compatible with that proposal.

Functional Cooperativity between Neural CAMs in Axon Outgrowth and Guidance

A variety of recognition and signaling mechanisms are thought to operate in a concerted fashion in the process of axon steering (Goodman, 1996). Cell adhesion and other related molecules probably mediate a substantial fraction of those mechanisms. The usual absence of severe phenotypes in loss-of-function mutants for any single relevant putative gene has been explained by the functional cooperation and partial overlapping of different guidance mechanisms (Goodman, 1996; Hynes, 1996). If so, appropriate double mutant combinations might be expected to result in synergistic phenoypes. This has indeed been the case in the few instances in which that hypothesis has been tested. Thus, double mutants for two *Drosophila* receptor tyrosine phosphatase genes, *Ptp69D* and *Ptp99A*, show a synergistic phenotype in motor neuron axon guidance (Desai et al., 1996). Also, a synergistic CNS phenotype was found in double mutants for the CAM gene *FasI* and the cytoplasmic tyrosine kinase *abl* gene, the latter thought to mediate intracellular signal transduction of adhesion or signaling receptor(s) (Elkins et al., 1990). In this paper, we have shown that synergistic CNS phenotypes are produced in double mutant embryos for *nrt* and *nrg* as well as *drl* and *kek1*. Since in several other double mutant combinations the phenotypes are simply additive, it is plausible to conclude that the former phenotypes are not simply due to a general, nonspecific, deleterious effect produced by the lack of Nrt. Likewise, the synergistic phenotypes strengthen the evidence for a role of Nrt during axogenesis within the CNS and also reveal the participation of the other three genes in the same process, a function not uncovered previously by the analysis of single mutant embryos (Bieber et al., 1989; Callahan et al., 1995; Musacchio and Perrimon, 1996; Hall and Bieber, 1997). Furthermore, the phenotypic synergy reported here is, to our knowledge, the first direct in vivo demonstration by genetic means of the existence of functional cooperation in the CNS between one CAM, Nrt, and other CAMs and receptor-like signaling molecules.

Although Nrg and Nrt are likely expressed in all CNS neurons during the critical stages of axogenesis, *nrg*$^-$; *nrt*$^-$ embryos display specific misguidance phenotypes (Figure 5). With the proviso that eventual heterogeneities in the expression of Nrg (and Nrt) might provide CNS axons with some guidance cues, we suggest that, in line with the hypothesis presented above to account for the guidance defects of *nrt*$^-$ single mutants, the concomitant lack of Nrt and Nrg can strongly weaken axon-to-axon interactions within any given fascicle, causing frequent loss of contact with their neighbors. Consequently, single axons might become prone to stall or leave their normal pathways of growth and, eventually, to join another pathway with the same "label." In addition, the analysis of a subset of identified neurons in *nrg*$^-$; *nrt*$^-$ embryos with mAb 22C10 has shown that certain axon projections do not seem to be affected, whereas others frequently display misguidance phenotypes. This suggests a degree of specificity in the requirements of particular axons for Nrg (and Nrt). Although Ptp69D and Ptp99A are, like Nrg, widely expressed in the CNS, we have not detected phenotypic synergy in their double mutant combinations with *nrt*. It is thus possible that differences exist in the relative requirements of different axonal pathways for the several molecules that operate during growth and guidance in the CNS but apparently have uniform distribution.

The putative transmembrane proteins encoded by the genes *kek1* and *kek2* show striking conservation of their extracellular domains to other known adhesion and signaling molecules and are coexpressed in many neurons (Musacchio and Perrimon, 1996). This had led some to propose that a redundant function of both proteins might explain the lack of an overt CNS phenotype in *kek1* null mutants (Musacchio and Perrimon, 1996). Nevertheless, since absolute gene redundancy is probably the exception in nature, it is more likely a situation of partial redundancy. Accordingly, the local axonal defasciculation in *kek1*$^-$ embryos and the synergistic phenotypes in *kek1*$^-$; *nrt*$^-$ embryos indicate that *kek2* cannot totally substitute for *kek1*. Therefore, *kek1* function must be regarded as unique.

Among the several double mutant combinations between *nrt* and other genes of highly restricted CNS expression that we have studied, only the *drl*$^-$; *nrt*$^-$ combination has resulted in a clear synergistic phenotype (Figures 6C–6E). The double mutant analysis has confirmed that Drl participates in the fasciculation and guidance of Drl-expressing axons, as already inferred from the phenotype of *drl*$^-$ single mutants (Callahan et al., 1995). Interestingly, guidance of other axons that do not express Drl, like those expressing Fas II, is also affected in *drl*$^-$; *nrt*$^-$ embryos (Figure 6E). Two possible interpretations could account for the phenotype of *drl*$^-$; *nrt*$^-$ embryos. (1) Drl signaling through recognition of its (unknown) ligand gives the Drl neurons guidance instructions that are partially redundant with another pathway involving Nrt. Thus, in *drl*$^-$ single mutants, mild phenotypes are observed, whereas in the double mutant guidance of Drl axons is highly abnormal. The nonautonomous misguidance of other axons in the CNS (such as the Fas II pathways) could then be interpreted as simply being due to the loss of a cellular guidance cue provided by Drl neurons. (2) This nonautonomous phenotype could alternatively reveal that Drl signaling is bidirectional, like that of membrane tyrosine kinases of the Eph family (Henkemeyer et al., 1996; Holland et al., 1996), and Drl activates its (unknown) receptor expressed on other neurons (such as the Fas II neurons). This signal would be redundant with an Nrt signal (this could come from neurons that do not express Drl, since all CNS neurons express Nrt). Thus, in the double mutant, these adjacent (Fas II$^+$) axons would display abnormal guidance. Future experiments, like the specific ablation of

Drl neurons, may allow us to distinguish between both interpretations. Phenotypic nonautonomy during CNS morphogenesis can also be inferred in other instances, as for *FasI* from the analysis of *Abl*$^{-}$ *Fas*$^{-}$ double mutant embryos reported by Elkins et al. (1990).

In summary, the analysis of *nrt* mutations, alone or in combination with mutations in the three other genes with functions presumed to be related, has demonstrated their requirement for axon outgrowth, fasciculation, and guidance. It follows that a complex and diverse functional cooperation among their gene products exists in the CNS. Future work should show whether mutations in other genes of widespread neural expression like *nrt* (e.g., *nrg*) behave similarly in double mutant combinations. This will help to understand better the complexity of interactions occurring during growth cone steering between the different functional pathways mediated by adhesion/signaling molecules.

Experimental Procedures

Genetic Methods and Mutagenesis

Males of the genotype *mwh jv st e* were mutagenized with 6 mM diepoxibutane, according to the method of Lewis and Bacher (1968). Mutagenized chromosomes were recovered over *TM3* balancer chromosomes in females. Groups of 50 such females were mated to *Df(3L)st*$^{81k17.2}$*/TM6B* males and their embryonic progeny stained with anti-Nrt mAb 43B5. Whenever embryos with low or no staining were observed, the group of 50 females was divided into five groups of 10 and the analysis repeated. If unstained embryos newly appeared in one group, stable lines were derived from each of the 10 females and the presence of a presumptive mutation in *nrt* was tested by staining embryos of each line. Out of 2500 mutagenized chromosomes analyzed in this way, one mutant allele, *nrt*^{1}, was isolated. The *nrt*^{1} chromosome, initially lethal, became viable after outcrossing it to a wild-type background.

The enhancer trap line *rP668* was a gift from the laboratory of G. Rubin. It contains a P-lArB element (Wilson et al., 1989) inserted at cytological position 73C1–2. To obtain excision revertants of the P element in *rP668*, the transposon was mobilized by crossing to flies carrying a stable source of transposase activity (Robertson et al., 1988). Excision lines were established that had lost the *rosy*$^{+}$ marker gene and examined for Nrt expression during embryogenesis using mAb 43B5. Several of those lines that showed no 43B5 antigen were analyzed molecularly and one of them, *nrt*^{5}, was used for subsequent studies. One excision line, *R20F*, where the wild-type pattern of Nrt expression had been restored, was used as a control. Alleles of other genes used for double mutant analysis were *nrg*^{1} and *nrg*^{2} (Hall and Bieber, 1997), *FasI*^{TE} and *FasIII*^{E25} (Elkins et al., 1990), *FasII*^{eB112} (Grenningloh et al., 1991), *nrm*^{48} and *Df(3L)ΔAK1* (Kania and Bellen, 1995), *plx*$^{\Delta 180}$ (Zhang et al., 1996), *kek1*^{RM2} and *kek1*^{RA5} (Musacchio and Perrimon, 1996), *drl*$^{P3.765}$ (Callahan et al., 1995), *Ptp69D*^{1} and *Df(3L)8ex25* (Desai et al., 1996), and *Ptp99A*^{1} (Hamilton et al., 1995). Other mutant strains are described in Lindsley and Zimm (1992).

The strains *GAL4*^{Mz1407} and *GAL4*^{Mz1277} (a gift from J. Urban), and *GAL4*$^{G537.4}$ (an insertion in *scabrous*; a gift from U. Hinz) were used to induce ectopic expression of Nrt. Transformant lines carrying a *UAS–nrt* insertion were produced using *nrt* cDNA B41 (de la Escalera et al., 1990) as indicated in Brand and Perrimon (1993).

Parental individuals for the analysis of double mutant progeny were obtained by the appropriate crosses or by recombination using, whenever necessary, balancer chromosomes carrying a *lacZ* insertion. For the analysis of *FasII*^{eB112}; *nrt*^{5} embryos, the parents also carried a marker second chromosome with an *ftz*$_{ng}$*-tau-*β*-gal* construct (Callahan and Thomas, 1994). This construct expresses β-gal in some axons that also express Fas II (Lin et al., 1994).

Genomic Cloning and Molecular Mapping

DNA clones were isolated from a genomic library (Maniatis et al., 1978) using an *nrt* cDNA as a probe. After restriction mapping, the cloned region was shown to encompass about 30 kb of DNA. Using *nrt* cDNA B41 and Southern blot analysis, the approximate location of the transcription start site(s) and the existence of a large intron could be detected. The transcription start site(s) was more precisely determined by primer extension and by S1 mapping using poly(A)+ RNA from 0- to 2-day-old pupae. At this stage, the two major *nrt* mRNAs are present in similar amounts. A single transcription start site was found, and the DNA region upstream to it was partially sequenced. The existence of consensus donor and acceptor splicing sequences (Keller and Noon, 1985) at the exon–intron boundaries of the large intron was determined by DNA sequencing.

To determine the nature of the *nrt*^{1} mutation at the molecular level, DNA from homozygous *nrt*^{1} flies was digested with appropriate restriction enzymes to obtain small fragments and, after Southern blotting, hybridized to cDNA B41. A small DNA deletion could thus be detected within the *nrt* coding region. The region containing the deletion was amplified by PCR and sequenced to determine the exact size of the deletion. As a control, parental *mwh jv st e* flies were used.

The approximate insertion site of the P transposon in the enhancer trap line *rP668* was determined by analyzing the restriction map of the *nrt* genomic region in homozygous *rP668* flies by Southern blot hybridization using genomic clones as probes. To determine the site of insertion precisely, *rP668* DNA was amplified by PCR using primers corresponding to the end of the transposon and to the surrounding *nrt* region. The amplified DNA was then sequenced. Southern blot analysis was used for restriction mapping to determine the approximate position of the breakpoints of the DNA deletion associated with the *nrt*^{5} allele, which was obtained by imprecise excision of the transposon.

Immunohistochemistry

Embryos raised at 25°C (29°C for the GAL4 rescue experiment) were fixed and stained as previously described (Carmena et al., 1995). Following HRP immunostaining, embryos were cleared and dissected in 50% glycerol and mounted in 100% glycerol for observation. Confocal images were obtained as in Carmena et al. (1995). Alternatively, fixed embryos were embedded in paraffin wax (Romani et al., 1987); sections (8 μm) were obtained, treated with xilene, and rehydrated. After incubation with anti-Nrt mAb 43B5 for 30 min, the sections were further treated in the same way as embryo whole mounts.

Double mutant embryos were identified by staining with mAb 43B5 alone (double mutant recombinants for *nrt* and *FasI*, *Ptp69D*, *Ptp99A*, or *nrm*), or together with mAbs (a gift from C. Goodman) against the appropriate proteins (double mutants for *nrt* and *nrg*, *FasII*, or *FasIII*), or with anti-β-gal antibodies (to detect the presence of that protein in marked balancer chromosomes in all other cases, in *drl*$^{P3.765}$, and in the chromosome bearing the *ftz*$_{ng}$*-tau-*β*-gal* construct).

Pupae were processed as previously described (García-Alonso et al., 1996) and stained with mAbs 22C10 or 43B5 followed by the appropriate biotinylated secondary antibody and the Elite kit (Vector).

Acknowledgments

We thank an anonymous reviewer for valuable suggestions to improve the Discussion; T. Kornberg for comments on the manuscript; K. Zinn for detailed information on *Ptp69D* alleles; and H. Bellen, J. Campos-Ortega, C. Goodman, W. Hinz, W. Odenwald, N. Perrimon, G. Rubin, J. Thomas, J. Urban, and K. Zinn for flies and antibodies. S. S. was supported by a contract from the Human Capital and Mobility Programme of the European Union. A. C., M. D. M.-B., and S. E. held fellowships from the Spanish Ministerio de Educacion y Cultura (M.E.C.). L. G.-A. was supported by a temporary contract from the Spanish M.E.C. This work was supported by grants from Spanish Direccion General de Investigacion Cientifica y Technica (PB93–0099) and the European Union (BIO4-CT96–0450) to F. J., and an institutional grant from Fundación Ramón Areces to the C.B.M.S.O.

Received July 16, 1997; revised December 11, 1997.

References

Auld, V.J., Fetter, R.D., Broadie, K., and Goodman, C.S. (1995). Gliotactin, a novel transmembrane protein on peripheral glia, is required to form the blood-nerve barrier in *Drosophila*. Cell *81*, 757–767.

Barthalay, Y., Hipeau-Jacquotte, R., de la Escalera, S., Jiménez, F., and Piovant, M. (1990). *Drosophila* neurotactin mediates heterophilic cell adhesion. EMBO J. *9*, 3603–3609.

Bieber, A.J., Snow, P.M., Hortsch, M., Patel, N.H., Jacobs, J.R., Traquina, Z.R., Schilling, J., and Goodman, C.S. (1989). *Drosophila* neuroglian: a member of the immunoglobulin superfamily with extensive homology to the vertebrate neural adhesion molecule L1. Cell *59*, 447–460.

Bossing, T., and Technau, G.M. (1994). The fate of the CNS midline in *Drosophila* as revealed by a new method for single cell labeling. Development *120*, 1895–1906.

Brady-Kalnay, S.M., and Tonks, N.K. (1995). Protein tyrosine phosphatases as adhesion receptors. Curr. Opin. Cell Biol. *7*, 650–657.

Brand, A.H., and Perrimon, N. (1993). Targeted gene expression as a means of altering cell fates and generating dominant phenotypes. Development *118*, 401–415.

Butler, S.J., Ray, S., and Hiromi, Y. (1997). *klingon*, a novel member of the *Drosophila* immunoglobulin superfamily, is required for the development of the R7 photoreceptor neuron. Development *124*, 781–792.

Callahan, C.A., and Thomas, J.B. (1994). Tau-β-galactosidase, an axon-targeted fusion protein. Proc. Natl. Acad. Sci. USA *91*, 5972–5976.

Callahan, C.A., Muralidhar, M.G., Lundgren, S.E., Scully, A.L., and Thomas, J.B. (1995). Control of neuronal pathway selection by a *Drosophila* receptor protein-tyrosine kinase family member. Nature *376*, 171–174.

Carmena, A., Bate, M., and Jiménez, F. (1995). *lethal of scute*, a proneural gene, participates in the specification of muscle progenitors during *Drosophila* embryogenesis. Genes Dev. *9*, 2373–2383.

Chiba, A., Snow, P., Keshishian, H., and Hotta, Y. (1995). Fasciclin III as a synaptic target recognition molecule in *Drosophila*. Nature *374*, 166–168.

Darboux, I., Barthalay, Y., Piovant, M., and Hipeau-Jacquotte, R. (1996). The structure-function relationships in *Drosophila* neurotactin show that cholinesterasic domains may have adhesive properties. EMBO J. *15*, 4835–4843.

de la Escalera, S., Bockamp, E.O., Moya, F., Piovant, M., and Jimenez, F. (1990). Characterization and gene cloning of Neurotactin, a *Drosophila* transmembrane protein related to cholinesterases. EMBO J. *9*, 3593–3601.

Desai, C.J., Gindhart, J.G., Jr., Goldstein, L.S.B., and Zinn, K. (1996). Receptor tyrosine phosphatases are required for motor axon guidance in the *Drosophila* embryo. Cell *84*, 599–609.

Desai, C.J., Krueger, N.X., Saito, H., and Zinn, K. (1997). Competition and cooperation among receptor tyrosine phosphatases control motoneuron growth cone guidance in *Drosophila*. Development *124*, 1941–1952.

Doe, C.Q., Hiromi, Y., Gehring, W.J., and Goodman, C.S. (1988a). Expression and function of the segmentation gene *fushi tarazu* during *Drosophila* neurogenesis. Science *239*, 170–175.

Doe, C.Q., Smouse, D., and Goodman, C.S. (1988b). Control of neuronal fate by the *Drosophila* segmentation gene *even-skipped*. Nature *333*, 376–378.

Doherty, P., and Walsh, F.S. (1994). Signal transduction events underlying neurite outgrowth stimulated by cell adhesion molecules. Curr. Opin. Neurobiol. *4*, 49–55.

Elkins, T., Zinn, K., MacAllister, L., Hoffmann, F.M., and Goodman, C.S. (1990). Genetic analysis of *Drosophila* neural cell adhesion molecule: interaction of *Fasciclin I* and *abelson tyrosine kinase* mutations. Cell *60*, 565–575.

Fashena, S.J., and Zinn, K. (1995). The ins and outs of receptor tyrosine phosphatases. Curr. Biol. *15*, 1367–1369.

Fujita, S.C., Zipurski, S.L., Benzer, S., Ferrús, A., and Shotwell, S.L. (1982). Monoclonal antibodies against the *Drosophila* nervous system. Proc. Natl. Acad. Sci. USA *79*, 7929–7933.

García-Alonso, L., Fetter, R.D., and Goodman, C.S. (1996). Genetic analysis of *Laminin A* in *Drosophila*: extracellular matrix containing laminin A is required for ocellar axon pathfinding. Development *122*, 2611–2622.

Goodman, C.S. (1996). Mechanisms and molecules that control growth cone guidance. Annu. Rev. Neurosci. *19*, 341–377.

Goodman, C.S., and Shatz, C.J. (1993). Developmental mechanisms that generate precise patterns of neuronal connectivity. Cell *72*/Neuron *10* (suppl.) 77–98.

Goodman, C.S., Bastiani, M.J., Doe, C.Q., du Lac, S., Helfand, S.L., Kuwada, J.Y., and Thomas, J.B. (1984). Cell recognition during neuronal development. Science *225*, 1271–1279.

Grenningloh, G., Bieber, A.J., Rehm, E.J., Snow, P.M., Traquina, Z.R., Hortsch, M., Patel, N.H., and Goodman, C.S. (1990). Molecular genetics of neuronal recognition in *Drosophila*: evolution and function of immunoglobulin superfamily cell adhesion molecules. Cold Spring Harbor Symp. Quant. Biol. *55*, 327–340.

Grenningloh, G., Rehm, E.J., and Goodman, C.S. (1991). Genetic analysis of growth cone guidance in *Drosophila*: Fasciclin II functions as a neuronal recognition molecule. Cell *67*, 45–57.

Hall, S.G., and Bieber, A.J. (1997). Mutations in the *Drosophila* neuroglian cell adhesion molecule affect motor neuron pathfinding and peripheral nervous system patterning. J. Neurobiol. *32*, 325–340.

Halter, D.A., Urban, J., Rickert, C., Ner, S.S., Ito, K., Travers, A.A., and Technau, G.M. (1995). The homeobox gene *repo* is required for the differentiation and maintenance of glia function in the embryonic nervous system of *Drosophila melanogaster*. Development *121*, 317–332.

Hamilton, B.A., Ho, A., and Zinn, K. (1995). Targeted mutagenesis and genetic analysis of a *Drosophila* receptor-linked protein tyrosine phosphatase gene. Roux's Arch. Dev. Biol. *204*, 187–192.

Henkemeyer, M., Orioli, D., Henderson, J.T., Saxton, T.M., Roder, J., Pawson, T., and Klein, R. (1996). Nuk controls pathfinding of commissural axons in the mammalian central nervous system. Cell *86*, 35–46.

Hinz, U., Giebel, B., and Campos-Ortega, J.A. (1994). The basic-helix-loop-helix of *Drosophila* lethal of scute protein is sufficient for proneural function and activates neurogenic genes. Cell *76*, 77–87.

Holland, S.J., Gale, N.W., Mbamalu, G., Yancopoulos, G.D., Henkemeyer, M., and Pawson, T. (1996). Bidirectional signalling through the EPH-family receptor Nuk and its transmembrane ligands. Nature *383*, 722–725.

Hortsch, M., Bieber, A., Patel, N., and Goodman, C.S. (1990a). Differential splicing generates a nervous system-specific form of *Drosophila* neuroglian. Neuron *4*, 697–709.

Hortsch, M., Patel, N.H., Bieber, A.J., Traquina, Z.R., and Goodman, C.S. (1990b). *Drosophila* neurotactin, a surface glycoprotein with homology to serine esterases, is dynamically expressed during embryogenesis. Development *110*, 1327–1340.

Hunter, D.D., Porter, B.E., Bulock, J.W., Adams, S.P., Merlie, J.P., and Sanes, J.R. (1989). Primary sequence of a motor neuron-selective adhesion site in the synaptic basal lamina protein S-laminin. Cell *59*, 905–913.

Hynes, R.O. (1996). Targeted mutations in cell adhesion genes: what have we learned from them? Dev. Biol. *180*, 402–412.

Hynes, R.O., and Lander, A.D. (1992). Contact and adhesive specificities in the associations, migrations, and targeting of cells and axons. Cell *68*, 303–322.

Ichtchenko, K., Hata, Y., Nguyen, T., Ullrich, B., Missler, M., Moomaw, C., and Südhof, T.C. (1995). Neuroligin 1: a splice site-specific ligand for β-Neurexins. Cell *81*, 435–443.

Ichtchenko, K., Nguyen, T., and Südhof, T.C. (1996). Structures, alternative splicing, and neurexin binding of multiple neuroligins. J. Biol. Chem. *271*, 2676–2682.

Jacobs, J.R., and Goodman, C.S. (1989). Embryonic development of axon pathways in the *Drosophila* CNS: I. A glial scaffold appears before the first growth cones. J. Neurosci. *9*, 2402–2411.

Jacobs, J.R., Hiromi, Y., Patel, N.H., and Goodman, C.S. (1989). Lineage, migration and morphogenesis of longitudinal glia in the *Drosophila* CNS as revealed by a molecular lineage marker. Neuron *2*, 1625–1631.

Kania, A., and Bellen, H.J. (1995). Mutations in *neuromusculin*, a gene encoding a cell adhesion molecule, cause nervous system defects. Roux's Arch. Dev. Biol. *204*, 259–270.

Keines, R., and Cook, G.M.W. (1995). Axon guidance molecules. Cell *83*, 161–169.

Keller, E.B., and Noon, W.A. (1985). Intron splicing: a conserved internal signal in introns of *Drosophila* pre-mRNAs. Nucleic Acids Res. *13*, 4971–4981.

Klämbt, C., Jacobs, J.R., and Goodman, C.S. (1991). The midline of the *Drosophila* central nervous system: a model for the genetic analysis of cell fate, cell migration, and growth cone guidance. Cell *64*, 801–815.

Lewis, E.B., and Bacher, F. (1968). Method of feeding ethyl methanesulfonate (EMS) to *Drosophila* males. Drosophila Inform. Serv. *43*, 193.

Lin, D.M., and Goodman, C.S. (1994). Ectopic and increased expression of Fasciclin II alters motoneuron growth cone guidance. Neuron *13*, 507–523.

Lin, D.M., Fetter, R.D., Kopczynski, C., Grenningloh, G., and Goodman, C.S. (1994). Genetic analysis of Fasciclin II in *Drosophila*: defasciculation, refasciculation, and altered fasciculation. Neuron *13*, 1055–1069.

Lindsley, D.L., and Zimm, G.G. (1992). The genome of *Drosophila melanogaster* (San Diego: Academic Press).

Maniatis, T., Hardinson, R.C., Lacy, E., Lauer, J., O'Connell, C., and Quon, D. (1978). The isolation of structural genes from libraries of eucaryotic DNA. Cell *15*, 687–701.

Müller, U., and Kypta, R. (1995). Molecular genetics of neuronal adhesion. Curr. Opin. Neurobiol. *5*, 36–41.

Musacchio, M., and Perrimon, N. (1996). The *Drosophila* kekkon genes: novel members of both the leucine-rich repeat and immunoglobulin superfamilies expressed in the CNS. Dev. Biol. *178*, 63–76.

Nose, A., Takeichi, M., and Goodman, C.S. (1994). Ectopic expression of Connectin reveals a repulsive function during growth cone guidance and synapse formation. Neuron *13*, 525–539.

Olson, P.F., Fessler, L.I., Nelson, R.E., Sterne, R.E., Campbell, A.G., and Fessler, J.H. (1990). Glutactin, a novel *Drosophila* basement membrane related glycoprotein with sequence similarity to serine esterases. EMBO J. *9*, 1219–1227.

Patel, N.H., Martín-Blanco, E., Coleman, K.G., Poole, S.J., Ellis, M.C., Kornberg, T.B., and Goodman, C.S. (1989). Expression of engrailed proteins in arthropods, annelids, and chordates. Cell *58*, 955–968.

Ramos, R.G.P., Igloi, G.L., Lichte, B., Baumann, U., Maier, D., Schneider, T., Brandstätter, J.H., Fröhlich, A., and Fiscbach, K.-F. (1993). The *irregular chiasm C-roughest* locus of *Drosophila*, which affects axonal projections and programmed cell death, encodes a novel immunoglobulin-like protein. Genes Dev. *7*, 2533–2547.

Robertson, H.M., Prestion, C.R., Phillis, R.V., Johnson-Schlitz, D.M., Benz, D.M., and Engels, W.R. (1988). A stable genomic source of P element transposase in *Drosophila melanogaster*. Genetics *118*, 461–470.

Romani, S., Campuzano, S., and Modolell, J. (1987). The *achaete-scute* complex is expressed in neurogenic regions of *Drosophila* embryos. EMBO J. *6*, 2085–2092.

Rutishauser, U. (1993). Adhesion molecules of the nervous system. Curr. Opin. Neurobiol. *3*, 709–715.

Seeger, M., Tear, G., Ferres-Marco, D., and Goodman, C.S. (1993). Mutations affecting growth cone guidance in *Drosophila*: genes necessary for guidance toward or away from the midline. Neuron *10*, 409–426.

Tanaka, E., and Sabry, J. (1995). Making the connection: cytoskeletal rearrangements during growth cone guidance. Cell *83*, 171–176.

Tian, S.-S., Tsoulfas, P., and Zinn, K. (1991). Three receptor-linked protein-tyrosine phosphatases are selectively expressed on central nervous system axons in the *Drosophila* embryo. Cell *67*, 675–685.

Wilson, C., Pearson, R.K., Bellen, H., O'Kane, C., Grossniklaus, U., and Gehring, W.J. (1989). P-element-mediated enhancer detection: an efficient method for isolating and characterizing developmentally regulated genes in *Drosophila*. Genes Dev. *3*, 1301–1313.

Yang, X., Seow, K.T., Bahri, S.M., Oon, S.H., and Chia, W. (1991). Two *Drosophila* receptor-like tyrosine phosphatase genes are expressed in a subset of developing axons and pioneer neurons in the embryonic CNS. Cell *67*, 661–673.

Zhang, S.D., Kassis, J., Olde, B., Mellerick, D.M., and Odenwald, W.F. (1996). Pollux, a novel *Drosophila* adhesion molecule, belongs to a family of proteins expressed in plants, yeast, nematodes, and man. Genes Dev. *10*, 1108–1119.

Zhong, Y., and Shanley, J. (1995). Altered nerve terminal arborization and synaptic transmission in *Drosophila* mutants of cell adhesion molecule Fasciclin I. J. Neurosci. *15*, 6679–6687.